

Heat Conduction in Star-Perforated Solid Propellant Grains

DONALD A. WILLOUGHBY*
Rohm & Haas Company, Huntsville, Ala.

A new method for the analysis of transient-state heat conduction problems for solid propellant grains having a general star-shaped internal perforation was developed. A conformal transformation is used to map transverse cross sections of star-perforated propellant grains onto an annulus. The two-dimensional heat conduction equation with associated boundary conditions is subjected to the same transformation and is written in explicit finite-difference form for solution on a digital computer. The solution of the transformed problem in the annulus and the correspondence of points between the two geometries provides a solution for the star geometry. Results of computations for the exothermic cure of a star-perforated grain with a capacitive inner boundary condition and a convective outer boundary condition are compared with a similar problem having convection on both boundaries. The cool-down history of a fully cured grain having convection on both boundaries is illustrated.

Nomenclature

A	= constant in reaction rate expression
B_i	= inner boundary
B_o	= outer boundary
c	= specific heat
C_j	= mapping coefficient
d	= outward normal to grain
E	= constant in reaction rate expression
g	= constant heat flux
h	= heat-transfer coefficient
ΔH	= heat of reaction
k	= thermal conductivity
l	= line in z plane
n	= number of axes of symmetry
N	= exponent in reaction rate expression
P	= cure fraction
P_f	= final cure fraction
Q^*	= rate of volumetric internal heat generation
R	= outer radius of propellant grain
t	= time
T	= temperature
x, y	= rectangular coordinates in z plane
z	= complex plane of propellant grain
ζ	= complex plane of annulus
λ	= line in ζ plane corresponding to l
μ	= propellant density
ρ, θ	= polar coordinates in ζ plane
ω	= a function of ζ
\mathcal{K}	= heat capacity of mandrel segment per unit axial length

Subscripts

i	= inside surface
o	= outside surface
e	= environment
j	= index for mapping coefficient

Introduction

SOLID propellant grains are subjected to complex thermal phenomena during curing, particularly when the cure is coupled to the heat conduction process by an exothermic chemical reaction. In addition, thermal gradients that result from changes in the environmental conditions of a fully cured grain produce thermal stresses and alter the ballistic characteristics of the motor. Therefore, it is important to be

able to predict the thermal history of the grain during cure and the thermal response of the grain to changes in the environment.

Theoretical analyses of the heat conduction problem in solid propellant grains are often based on a one-dimensional approximation of the grain using a hollow circular cylinder of infinite length. Finite-difference methods are commonly used to solve the resulting problem, particularly when it is complicated by nonlinearities, complex boundary conditions, coupled chemical reactions, or simultaneous diffusion processes. However, in many practical cases the one-dimensional model is inadequate to describe the physical problem.

The finite-difference method is also applicable to the two-dimensional problem posed by the star perforation, but difficulties are encountered by the tendency of the grain boundaries to intersect coordinate lines. The difficulty has been handled in the past by writing special finite-difference equations for the intersections, by dividing the grain geometry into irregular segments and writing an approximate finite-difference relation for each segment, or by using an approximate grain geometry that is compatible with polar coordinates.

A new approach is to use the method of conformal mapping to obtain a coordinate system compatible with the boundaries of the star-perforated grain. A conformal transformation is used to map an annulus onto the star-perforated grain geometry. The polar coordinate system in the annulus maps onto a system of orthogonal curvilinear coordinates compatible with the grain boundaries. The equations describing the heat conduction problem are subjected to the same transformation. The transformed equations can be thought of as applying to the curvilinear coordinate system in the star-perforated grain geometry or to the polar coordinate system in the annulus. It has been found to be more convenient to work with the annulus, the solution of the transformed problem in the annulus and the correspondence of points between the two geometries providing the solution for the star geometry. The solution is found by writing the transformed problem in explicit finite-difference form and solving the resulting algebraic equations on an electronic digital computer. The analysis is generally applicable since a satisfactory mapping can be obtained for most star perforations.

Conformal Transformation

The conformal transformation described below may be used to map an annulus onto the transverse cross section of a star-perforated solid propellant grain. Figure 1 shows a segment of a typical annular region and a corresponding segment of the grain cross section bounded by lines of symmetry of the grain geometry.

Received March 6, 1964; revision received August 6, 1964. This work was supported by U. S. Army Contract No. DA-01-021-AMC-10037(Z).

* Intermediate Scientist, Applied Thermodynamics Group, Engineering Research Section, Redstone Arsenal Research Division. Member AIAA.

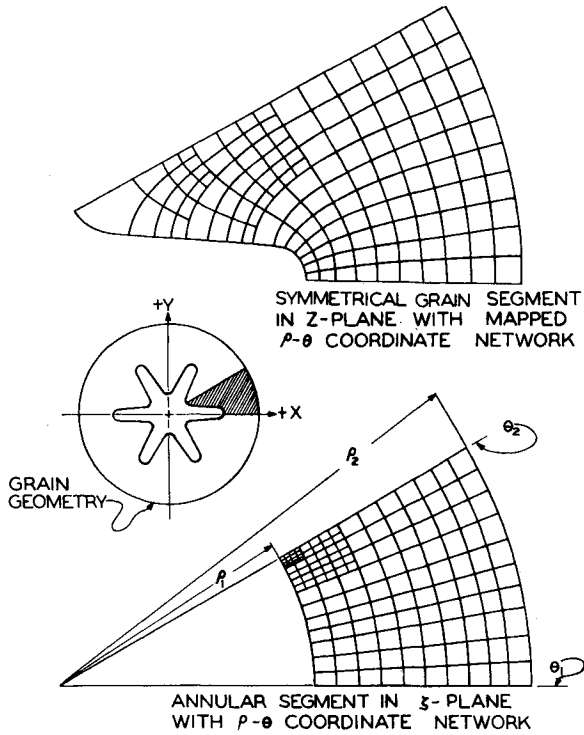


Fig. 1 Mapping of annular segment in ζ plane onto grain segment in z plane.

A mapping function of the form

$$z = \omega(\zeta) = \sum_{j=0}^m C_j \zeta^{1-n_j} \quad (1)$$

where C_0, \dots, C_m are real constants and C_0 is positive, can be used to obtain a conformal transformation of the region exterior to the unit circle in the complex ζ plane onto the region exterior to a closed star-shaped curve with n axes of symmetry in the complex z plane. The circle $|\zeta| = 1$ is mapped onto the star-shaped boundary; for $|\zeta| > 1$, the circle $|\zeta| = R/C_0$ is mapped onto an approximation of the circle $|z| = R$. As $|\zeta|$ increases, the approximation improves. Thus, the annular region is mapped onto the geometry of a star-perforated propellant grain with an outer radius R . Mapping coefficients C_j for particular grain designs may be

obtained by using a computer program described previously.¹ One hundred coefficients were used to map the grain shown in Fig. 1. The maximum deviation of the outer boundary from circularity is less than 1% of the outer radius.

Points on the complex z plane ($z = x + iy$) are related to points on the complex ζ plane ($\zeta = \xi + i\eta = \rho e^{i\theta}$) by Eq. (1). The following relationships may be obtained for the x and y coordinates:

$$x = \sum_{j=0}^m C_j \rho^{1-n_j} \cos(\theta - n_j \theta) \quad (2)$$

$$y = \sum_{j=0}^m C_j \rho^{1-n_j} \sin(\theta - n_j \theta) \quad (3)$$

The positive x axis is an axis of symmetry through the star point and corresponds to the angle $\theta = 0$.

If l represents any line in the z plane and λ represents the corresponding line in the ζ plane, it can be shown that²

$$\partial \lambda / \partial l = 1 / |\omega'(\zeta)| \quad (4)$$

The function $|\omega'(\zeta)|$ is called the stretching coefficient since it relates infinitesimal distances in the ζ plane to infinitesimal distances in the z plane. The function $|\omega'(\zeta)|^2 = |dz/d\zeta|^2$, which may be obtained from Eq. (1), is given by

$$|\omega'(\zeta)|^2 = \left[\sum_{j=0}^m C_j [1 - n_j] \rho^{-n_j} \cos(n_j \theta) \right]^2 + \left[\sum_{j=0}^m C_j [1 - n_j] \rho^{-n_j} \sin(n_j \theta) \right]^2 \quad (5)$$

When d represents the outward normal to the grain in the z plane, it can be shown that

$$\frac{\partial}{\partial d} = - \frac{1}{|\omega'(\zeta)|} \frac{\partial}{\partial \rho} \quad (6)$$

on an internal boundary and

$$\frac{\partial}{\partial d} = \frac{1}{|\omega'(\zeta)|} \frac{\partial}{\partial \rho} \quad (7)$$

on an external boundary.

Transformation of the Heat Conduction Problem

The conformal transformation described previously establishes a correspondence between points in the grain geometry

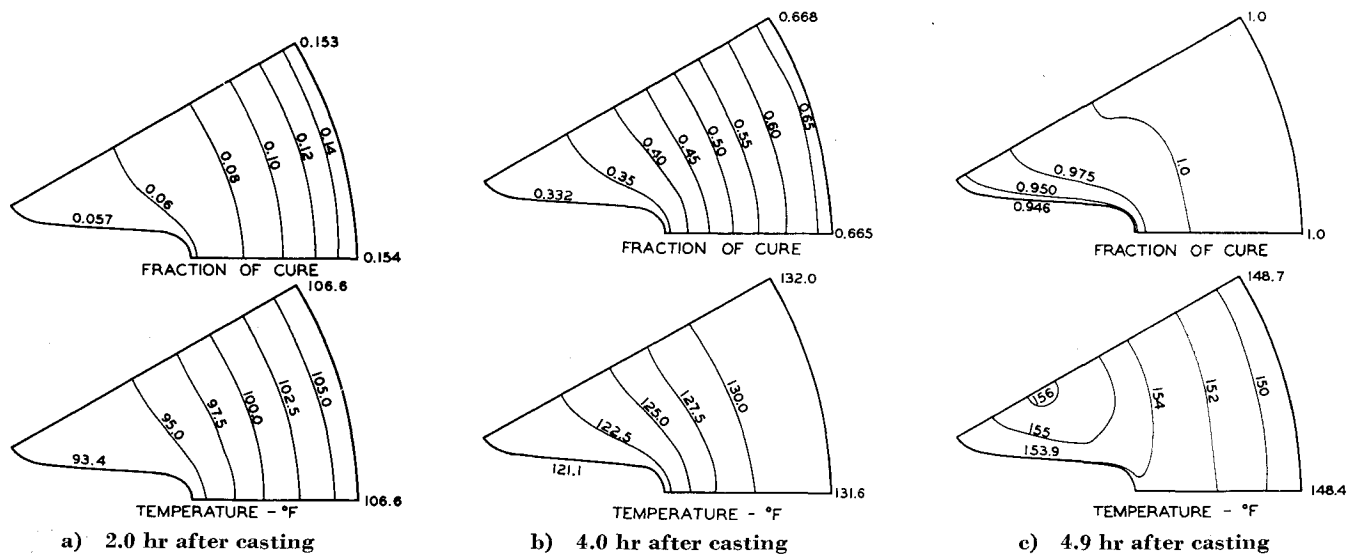


Fig. 2 Curing history for illustrative problem I.

Table 1 Boundary conditions

Condition ^a	Equation for z plane ^b	Equations for ζ plane ^c
Convective		
Inside	$\partial T/\partial d = h_i(T_e - T)/k$	$\partial T/\partial \rho = - \omega' h_i(T_e - T)/k$
Outside	$\partial T/\partial d = h_o(T_e - T)/k$	$\partial T/\partial \rho = + \omega' h_o(T_e - T)/k$
Constant Flux		
Inside	$\partial T/\partial d = g_i/k$	$\partial T/\partial \rho = - \omega' g_i/k$
Outside	$\partial T/\partial d = g_o/k$	$\partial T/\partial \rho = + \omega' g_o/k$
Capacitive		
Inside	$\int k(\partial T/\partial d)dB_i = -\mathcal{H}_i\partial T/\partial t$	$\int k(\partial T/\partial \rho)_\rho d\theta = \mathcal{H}_i\partial T_i/\partial t$
Outside	$\int k(\partial T/\partial d)dB_o = -\mathcal{H}_o\partial T/\partial t$	$\int k(\partial T/\partial \rho)_\rho d\theta = -\mathcal{H}_o\partial T_o/\partial t$

^a For inside, $B = B_i$, $\rho = \rho_i$; for outside, $B = B_o$, $\rho = \rho_o$.

^b $T_e = T_e(t)$; $T = T(x, y, t)$.

^c $T_e = T_e(t)$; $T = T(\rho, \theta, t)$, except for capacitive conditions, $T = T(\rho, t)$; $|\omega'| = |\omega'(\zeta)|$.

and the simpler annular geometry. The heat conduction equation with its associated boundary conditions is subjected to the same transformation, and the resulting equations are then written in finite-difference form for solution on a digital computer. The solution of the transformed problem in the annulus along with the correspondence of points between the two geometries provides a solution for the star geometry. The heat conduction equation with constant thermal properties was selected for use with the conformal transformation, since experience has shown that a significant reduction in computational effort over that required for variable thermal properties is obtained.

Heat Conduction Equations

The heat conduction equation written for constant thermal properties in rectangular (x, y) coordinates is

$$k \left[\frac{\partial^2 T}{\partial x^2} + \frac{\partial^2 T}{\partial y^2} \right] = \mu c \frac{\partial T}{\partial t} - Q^* \quad (8)$$

where k is thermal conductivity, T is temperature, μ is density, c is specific heat, t is time, and Q^* is the rate of volumetric internal heat generation. Equation (8), which applies to the z plane, may be transformed to the ζ plane by a change of variables described by Eq. (1). Procedures for accomplishing this transformation are described in standard works.^{3, 4} The heat conduction equation in polar (ρ, θ) coordinates in the ζ plane becomes

$$\frac{k}{|\omega'(\zeta)|^2} \left[\frac{\partial^2 T}{\partial \rho^2} + \frac{1}{\rho} \frac{\partial T}{\partial \rho} + \frac{1}{\rho^2} \frac{\partial^2 T}{\partial \theta^2} \right] = \mu c \frac{\partial T}{\partial t} - Q^* \quad (9)$$

For a curing reaction, the internal heat generation term is given by the equation

$$Q^* = \mu \Delta H \partial P / \partial t \quad (10)$$

where P is the fraction of cure and ΔH is the heat of reaction on curing. In many problems of practical importance, a general N th order curing reaction with an Arrhenius rate constant may be used to describe the cure:

$$\partial P / \partial t = A [P_f - P]^N \exp(-E/T_{abs}) \quad (11)$$

where A , E , P_f , and N are constants.

Initial and Boundary Conditions

No special transformation is required for initial conditions or for boundary conditions which specify temperature. However, the proper correspondence between points in the z plane and points in the ζ plane must be maintained.

Heat flux and convective boundary conditions specify a temperature gradient normal to the boundaries. Table 1

gives the boundary conditions as written for the grain geometry and as transformed to the annulus; B designates a boundary, subscripts i and o designate inner and outer boundaries, respectively, subscript e designates the environment, d is the outward normal to a surface of the star-perforated grain, and g represents a constant heat flux. The capacitive boundary condition involves an integration of the heat transfer to an adjacent material in perfect thermal contact having heat capacity \mathcal{H} per unit axial length and a very large thermal conductivity compared to that of the propellant.

Numerical Solution

The grids formed by the (ρ, θ) coordinates of the ζ plane map into curvilinear squares in the z plane as can be seen in Fig. 1. In order to obtain consistent accuracy of calculations throughout the grain and reasonable efficiency of total computation effort, it is necessary for the curvilinear squares in the z plane to be approximately uniform in size. This objective is accomplished by subdividing the grid structure in areas of relatively large stretching. Two subdivisions in grid size are adequate to obtain nearly uniform grids for mappings of most star-perforated propellant grains. Grids are subdivided by halving the grid size.

By use of a forward difference in time for the curing rate given by Eq. (11), the polymer fraction at each new time increment may be obtained as follows:

$$P(\rho, \theta, t + \Delta t) = P(\rho, \theta, t) + \Delta t \{ A [P_f - P]^N \exp(-E/T_{abs}) \} \quad (12)$$

Appropriate tests must be made to insure that P does not exceed P_f .

By use of a forward-difference approximation for the time derivative, and by use of central-difference approximations for the space derivatives, the following explicit finite-difference

Table 2 Data for problem I (Fig. 2) for curing from $P = 0$ to $P_f = 1.0$

Propellant:	
c	0.295 Btu/lb-°F
k	0.256 Btu/hr-ft-°F
ρ	111.5 lb/ft ³
\mathcal{H} for star-shaped aluminum mandrel	1.52 Btu/ft-°F
$T(t = 0)$, propellant, mandrel, and case	80.0°F
T_e (air oven)	130.0°F
h_o	1.0 Btu/hr-ft ² -°F
Motor o.d.	7.2 in.
ΔH , heat of curing	20.2 Btu/lb
Constants for Eq. (12):	
A	5.5625×10^{17} /hr
E	2.4234×10^4 °F
N	0.6

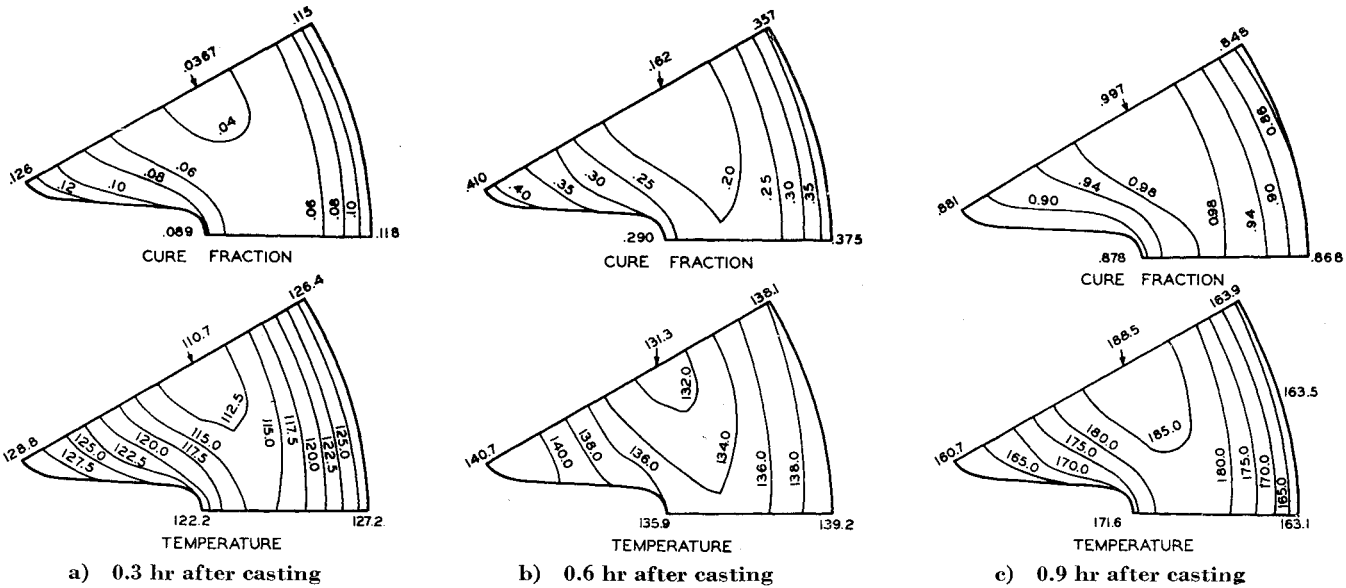


Fig. 3 Curing history for illustrative problem II.

equation can be obtained from Eq. (9) for interior nodal points:

$$T(\rho, \theta, t + \Delta t) = \frac{\Delta tk}{\mu c |\omega'(\rho, \theta)|^2} \times \left\{ \left[\frac{1 + (\Delta \rho / 2\rho)}{[\Delta \rho]^2} \right] T(\rho + \Delta \rho, \theta, t) + \left[\frac{1 - (\Delta \rho / 2\rho)}{[\Delta \rho]^2} \right] T(\rho - \Delta \rho, \theta, t) + \frac{1}{\rho^2 [\Delta \theta]^2} [T(\rho, \theta + \Delta \theta, t) + T(\rho, \theta - \Delta \theta, t)] \right\} + \left\{ 1 - \left[\frac{2 \Delta tk}{\mu c |\omega'(\rho, \theta)|^2} \right] \left[\frac{1}{[\Delta \rho]^2} + \frac{1}{\rho^2 [\Delta \theta]^2} \right] \right\} T(\rho, \theta, t) + \frac{\Delta H}{c} [P(\rho, \theta, t + \Delta t) - P(\rho, \theta, t)] \quad (13)$$

A detailed description of the numerical technique used and all of the finite-difference equations for the various boundary conditions are given in Ref. 5. This reference includes a discussion of stability and accuracy, a listing of the IBM 7090 FORTRAN computer program, and instructions for using the program. A limited number of copies of this report is available from the author upon request.

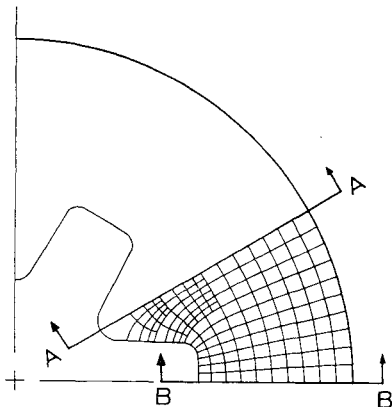


Fig. 4 Cross section of motor for illustrative problem III with mapped ρ - θ coordinate network.

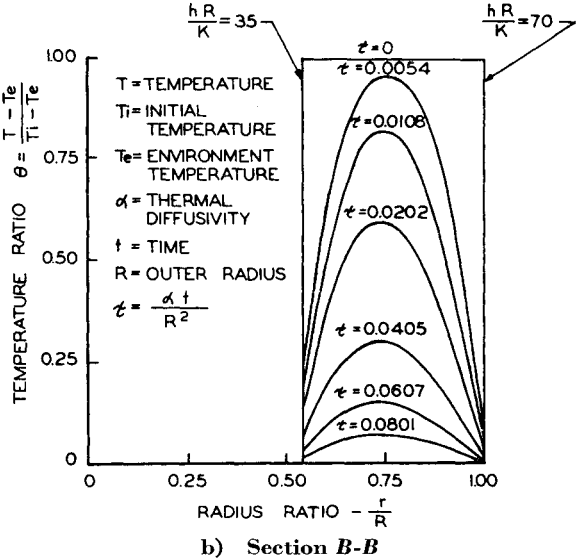
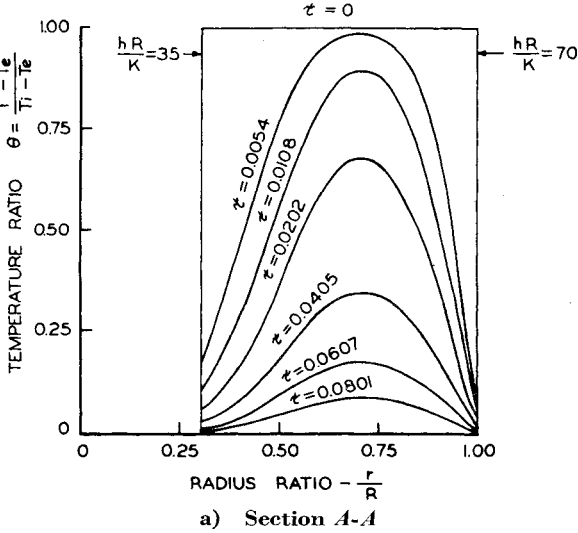


Fig. 5 Thermal history for problem III (see Fig. 4).

Illustrative Problems

For the first illustrative problem, consider the cure of a cylindrical motor with a six-pointed star perforation in which the end effects are negligible. A solid aluminum mandrel whose conductivity is very large compared to that of propellant forms the star-shaped perforation. A thermally thin metal case forms the outer boundary of the motor. The motor is assumed to be cast instantaneously with an exothermic chemical reaction starting immediately upon casting. The mandrel, the case, and the propellant are assumed to be at the same constant initial temperature. Immediately after casting, the outer surface of the motor is heated by the air environment in the curing oven. The mathematical model then consists of a star-perforated grain with a capacitive inner boundary condition and a convective outer boundary condition. Data for the problem are listed in Table 2.

A symmetrical segment of the motor with the finite-difference network that was used in the computations is shown in Fig. 1. Results of the computations are presented as contour maps of temperature and fraction of cure at selected times in Fig. 2. In Fig. 2a the outer surface is heated by the 130°F environment, which initiates the cure from the outside inward. This trend continues in Fig. 2b to the point where the cure is about two-thirds complete on the outer surface and about one-third complete on the inner surface. The final phase of the cure is characterized by a high-temperature region in the interior of the grain (Fig. 2c). The capacitive effect of the mandrel and the cooling effect of the environment have limited the temperature rise of the propellant near the surfaces.

The second example is similar to the first except for different initial and boundary conditions: $T(t = 0)$ of the grain = 100°F, $T_e = 140°F$, and a convective boundary condition is assumed for both the inside and outside boundaries, $h_i = h_o = 5 \text{ Btu/hr-ft}^2\text{-°F}$. Otherwise the problem is the same as the first example. Results of the computations are presented as contour maps of temperature and fraction of cure at selected times in Fig. 3. In Fig. 3a the cure has been initiated from both surfaces inward by heating from the higher

temperature environment. This trend continues in Fig. 3b with the surface approaching the environment temperature at 0.6 hr. At this point, the cure is progressing inward from the surfaces, but a relatively uncured region remains in the center of the web. In the Fig. 3c the rapid curing in the center of the web has resulted in a high-temperature region in this area; the temperature on the surface has been limited by heat transfer with the environment, which is at a lower temperature at this time.

The third example considers the thermal response of a star-shaped grain with convective heat transfer on the inside and outside boundaries. The motor is assumed to be at an initial uniform temperature and then suddenly exposed to a different constant environment temperature. Biot moduli of 35 and 70 were chosen for the inside and outside, respectively. A cross section of the motor is shown in Fig. 4 with the mapped coordinate lines used in the calculations indicated on the figure. The thermal history of section A-A in Fig. 4 is given in Fig. 5a, and the thermal history of section B-B in Fig. 4 is given in Fig. 5b. The rapid thermal response of the grain surface indicated in Fig. 5 is a result of the large Biot moduli. Results of this example are expressed in dimensionless form since the extremely nonlinear curing process is not present.

References

- ¹ Wilson, H. B., Jr., "A method of conformal mapping and the determination of stresses in solid propellant rocket grains," Rohm & Haas Co., Rept. S-38 (April 1963).
- ² Nehari, Z., *Conformal Mapping* (McGraw-Hill Book Co., Inc., New York, 1952), pp. 148-150.
- ³ Wylie, C. R., Jr., *Advanced Engineering Mathematics* (McGraw-Hill Book Co., Inc., New York, 1960), 2nd Ed., pp. 628-630.
- ⁴ Kantorovich, L. V. and Krylov, V. I., *Approximate Methods of Higher Analysis* (Interscience Publishers, Inc., New York, 1958), Chap. V, p. 358.
- ⁵ Willoughby, D. A., "Heat conduction in star-perforated solid propellant grains," Rohm & Haas Co., Rept. P-63-20 (November 1963).